substance: boron compounds with lanthanides
property: properties of lanthanide dodecaborides

Structure

The crystalline structure can be described in two ways

a) Metal atoms and cubooctahedral B_{12} units are arranged in a cubic face-centered lattice (Fig. 1a).

b) B_{24} cages surround the metal atoms which are arranged in a cubic lattice (Fig. 1b) [72S, 75S, 76C, 77M, 81S, 77S1, 77S2].

TbB_{12}

entropy

S	130(13) J mol^{-1}K^{-1}	86B

magnetic susceptibilities, Curie-Weiss constants, effective magnetic moments and pararnagnetic Curie points

χ_m	7770 cm^3/mol	T = 300 K	CGS-emu	73O
C_m	7.4 cm^3 K/mol			
p_{eff}	7.70 μ_B			
θ_p	– 652 K			

DyB_{12}

lattice parameters
(in Å)

a	7.5002(6)	T = 300 K	powder	91P
	7.5000(4)		beginning of the zone-melted rod	
	7.4999(3)		end of the zone-melted rod	

resistivity

ρ	25.56 µΩ cm	T = 300 K	94P
	2.678 µΩ cm	T = 4.2 K	

Temperature dependence of the electrical resistivity in Fig. 2A [98G, 99G].

magnetic properties

Néel temperature (T_N*, obtained from magnetic measurements; T_N**, obtained from resistivity measurements), paramagnetic Curie temperature Θ_p, effective magnetic moment p_{eff} (exp) and p_{eff} (theor)

T_N*	16.5 K			98G,
T_N**	16.44 K			99G
Θ_p	26.3 K			
p_{eff} (exp)	10.6 µ$_B$			
p_{eff} (theor)	10.63 µ$_B$			
T_N	16.44 K			94P
χ_m	38300 cm^3/mol	T = 300 K	magnetic susceptibility, CGS-emu	73O
C_m	12.3 cm^3 K/mol		Curie-Weiss constant	
p_{eff}	9.90 μ_B			
Θ_p	– 21 K			

entropy

S	138(13) J $mol^{-1}K^{-1}$	86B

HoB_{12}

lattice parameters
(in Å)

a	7.4916(10)	T = 300 K	powder	91P
	7.4923(3)		beginning of the zone-melted rod	
	7.4923(2)		end of the zone-melted rod	

resistivity

ρ	13.18 μΩ cm	T = 300 K	94P
	1.417 μΩ cm	T = 4.2 K	

Temperature dependence of resistivity in Fig. 3 [94P].

Temperature dependence of the electrical resistivity in Fig. 4 [98G, 99G].

magnetic properties

Néel temperature (T_N*, obtained from magnetic measurements; T_N**, obtained from resistivity measurements), paramagnetic Curie temperature Θ_p, effective magnetic moment p_{eff} (exp) and p_{eff} (theor)

T_N*	7.5 K			98G,
T_N**	7.36 K			99G
Θ_p	24.3 K			
p_{eff} (exp)	10.5 μ_B			
p_{eff} (theor)	10.60 μ_B			
T_N	7.36 K			94P
χ_m	44370 cm^3/mol	T = 300 K	magnetic susceptibility, CGS-emu	73O
C_m	13.8 cm^3 K/mol		Curie-Weiss constant	
p_{eff}	10.50 μ_B			
Θ_p	– 11 K			

Temperature dependence of the molar susceptibility in Fig. 5 [94P].

entropy

S	138(13) J $mol^{-1}K^{-1}$	86B

ErB_{12}

Structure investigation (boron-rich corner of the Er-Al-B system) in [94Y].

lattice parameters
(in Å)

a	7.4839(2)	T = 300 K	powder	91P
	7.4841(2)		beginning of the zone-melted rod	
	7.4837(3)		end of the zone-melted rod	

resistivity

ρ	12.40 μΩ cm	T = 300 K		94P
	0.711 μΩ cm	T = 4.2 K		

Temperature dependence of the electrical resistivity in Figs.3 [94P] and 6 [98G, 99G].

magnetic properties

Néel temperature (T_N*, obtained from magnetic measurements; T_N**, obtained from resistivity measurements), paramagnetic Curie temperature Θ_p, effective magnetic moment p_{eff} (exp) and p_{eff} (theor)

T_N*	6.7 K			98G,
T_N**	6.65 K			99G
Θ_p	14.6 K			
p_{eff} (exp)	9.5 μ_B			
p_{eff} (theor)	9.59 μ_B			
T_N	6.65 K			94P
χ_m	38550 cm^3/mol	T = 300 K	magnetic susceptibility, CGS-emu	73O
C_m	12.8 cm^3 K/mol		Curie-Weiss constant	
p_{eff}	10.10 μ_B			
Θ_p	– 32 K			

entropy

S	134(13) J $mol^{-1}K^{-1}$			86B

TmB_{12}

lattice parameters
(in Å)

a	7.4760(2)	T = 300 K	powder	91P
	7.4758(5)		beginning of the zone-melted rod	
	7.4752(2)		end of the zone-melted rod	

resistivity

ρ	14.04 μΩ cm	T = 300 K		94P
	1.589 μΩ cm	T = 4.2 K		

Temperature dependence of resistivity in Fig. 3 [94P].

Anisotropy of the temperature dependence of the electrical conductivity in Fig. 7 [98G, 99G].

magnetic properties

Néel temperature (T_N*, obtained from magnetic measurements; T_N**, obtained from resistivity measurements), paramagnetic Curie temperature Θ_p, effective magnetic moment p_{eff} (exp) and p_{eff} (theor)

T_N*	3.4 K			98G,
T_N**	3.28 K			99G
Θ_p	14.4 K			
p_{eff} (exp)	7.0 μ_B			
p_{eff} (theor)	7.57 μ_B			
T_N	3.28 K			94P
χ_m	25850 cm^3/mol	T = 300 K	magnetic susceptibility, CGS-emu	73O
C_m	9.0 cm^3 K/mol		Curie-Weiss constant	
p_{eff}	8.50 μ_B			
Θ_p	– 48 K			

entropy

S	138(13) J $mol^{-1}K^{-1}$	86B

YbB_{12}

Valence state of ytterbium in the dodecaboride [79M2].

Temperature dependence of the thermal expansion and expansion coefficient in Fig. 8 [87W].

Temperature dependence of the magnetic susceptibility in Fig. 9 [87W].

FIR reflectivity spectrum at 7 and 300 K in Fig. 10 [87W].

For physical properties see also [88S].

entropy

S	121(13) J $mol^{-1}K^{-1}$	86B

magnetic susceptibilities, Curie-Weiss constants, effective magnetic moments and pararnagnetic Curie points

χ_m	6820 cm^3/mol	T = 300 K	CGS-emu	73O
C_m	5.6 cm^3 K/mol			
p_{eff}	6.70 μ_B			
θ_p	– 520 K			

LuB_{12}

lattice parameters
(in Å)

a	7.4644(2)	T = 300 K	powder	91P
	7.4645(2)		beginning of the zone-melted rod	
	7.4644(2)		end of the zone-melted rod	

resistivity

ρ	11.51 μΩ cm	T = 300 K	94P
	0.160 μΩ cm	T = 4.2 K	

Temperature dependence of resistivity in Fig. 3 [94P].

Temperature dependence of the resistivity in Fig. 11 [95B, 98G, 99G].

Quantum oscillations and the Fermi surface of LuB_{12} in [95H].

critical temperature of superconductivity

T_c	0.48 K	91F, 68M

entropy

S	113(13) J $mol^{-1}K^{-1}$			86B

magnetic susceptibilities

χ_m	2896 cm^3/mol	T = 300 K	CGS-emu	73O

On magnetic properties, see also [77B2, 79M1].

Er-Cr-B system

Study of phase equilibria and crystalline structure of the ternary compounds in the Er-Cr-B system [86C].

Er-Al-B system

Structure investigation (boron-rich corner of the Er-Al-B system) in [94Y].

References:

68M Matthias, B.T., Geballe, T.H., Andres, K., Corenzwit, E., Hull, W., Maita, J.P.: Science 159 (1968) 530.

72S Schwetz, K., Ettmayer, P., Kieffer, R., Lipp, A.: Radex-Rundschau 3/4 (1972) 257.

73O Odintsov, V. V., Kostetskii, I. I., L'vov, S. N.: Izv. Akad. Nauk, Neorg. Mater. 9 (1973) 944: (engl. Transl. in Inorganic materials).

75S Samsonov, G.V., Serebryakova, T.I., Neronov, V.A.: in: Boridy, Moskva Atomzidat, 1975.

76C Condon, J.B.: C.E., Johnson, D.H., Steckel, L.M., : Inorg. Chem. 15 (1976) 2173.

77B1 Berezin, A. A., Golikova, O. A., Zaitsev, V. R., Kazanin, M. M., Orlov, V. M., Tkalenko, E. N., in:Boron and Refractory Borides, (Matkovich V. 1., ed.) Springer: Berlin, Heidelberg, New York 1977, p. 52.

77B2 Busehow, K. H. J.: see [77B1], p. 494.

77M Matkovich, V.I., Economy, J.: in: Boron and Refractory Borides, V.I. Matkovich ed., Springer: Berlin, 1977, p. 78.

77S1 Samsonov, G. V., Kovenskaya, B. A.: see [77B1], p. 5.

77S2 Samsonov, G.V., Kovenskaya, B.A.: in: Boron and Refractory Borides, V.I. Matkovich ed., Springer: Berlin, Heidelberg, New York, 1977, p. 5.

79M1 Moiseenko, L.L., Odintsov, V.V.: J. Less-Common Met. 67 (1979) 237.

79M2 Moiseenko, L.L., Odintsov, V.V., Grushko, Yu.S.: Inorg. Mater. 15 (1979) 542.

81S Schwetz, K.A., Reinmuth, K., Lipp, A.: Radex-Rundschau (1981) 568.

86B Borovikova, M.S., Fesenko, V.V.: J. Less-Common Met. 117 (1986) 287. (Proc. 8th Int. Symp. Boron, Borides, Carbides, Nitrides and Rel. Compounds, Tbilisi, Oct. 8 - 12, 1984)

86C Chaban, N.F., Datsyna, V.N.: Sov. Powder Metall. Met. Ceram. 25 (1986) 52.

87W Wachter, P.: in: Proc. 9th Int. Symp. Boron, Borides and Rel. Compounds, University of Duisburg, Germany, Sept. 21 - 25, 1987, H. Werheit ed., University of Duisburg: Duisburg, 1987, p. 166.

88S Sugiyama, K., Iga., F., Kasaya, M., Kasuya, T., Date, M.: J. Phys. Soc. Jpn. 57 (1988) 3946.

91F Fisk, Z.: in: Boron-Rich Solids, Proc. 10th Int. Symp. Boron, Borides and Rel. Compounds, Albuquerque, NM 1990 (AIP Conf. Proc. 231), D. Emin, T.L. Aselage, A.C. Switendick, B. Morosin, C.L. Beckel ed., American Institute of Physics: New York, 1991, p. 155.

91P Paderno, Yu.B., Filippov, V., Shitsevalova, N.: in: Boron-Rich Solids, Proc. 10th Int. Symp. Boron, Borides and Rel. Compounds, Albuquerque, NM 1990 (AIP Conf. Proc. 231), D. Emin, T.L. Aselage, A.C. Switendick, B. Morosin, C.L. Beckel ed., American Institute of Physics: New York, 1991, p. 460.

94P Paderno, Y., Paderno, V., Filippov, V.: Proc. 11th Int. Symp. Boron, Borides and Rel. Compounds, Tsukuba, Japan, August 22 - 26, 1993, Jpn. J. Appl. Phys. Series 10 (1994), p. 190.

94Y Yu, Y., Lundström, T.: J. Alloys Compounds 210 (1994) 191.

95B Bat'ko, I., Bat'kova, M., Flachbart, K., Filippov, V.B., Paderno, Yu.B., Shicevalova, N.Yu., Wagner, Th.: J. Alloys Compounds 217 (1995) L1.

95H Heinecke, M., Winzer, K., Noffke, J., Kranefeld, H., Grieb, H., Flachbart, K., Paderno, Yu.B.: Z. Phys. B 98 (1995) 231.

98G Gabani, S., Bat'ko, I., Flachbart, K., Shitsevalova, N., Paderno, Y., Herrmannsdorfer, T., Koenig, R.: Acta Phys. Slovaca 47 (1998) 755.

99G Gorshunov, B., Sluchanko, N., Volkov, A., Dressel, M., Knebel, G., Loidl, A., Kunii, S.: Phys. Rev . B 59 (1999) 1808.

Fig. 1.

Lanthanide dodecaborides. a) Structure model; metal atoms and cubo-octahedral B_{12} units arranged in a NaCl–like cubic face-centered lattice. b) Structure model; metal atoms arranged in a cubic lattice, each metal atom surrounded by a B_{24} cage [72S, 81S].

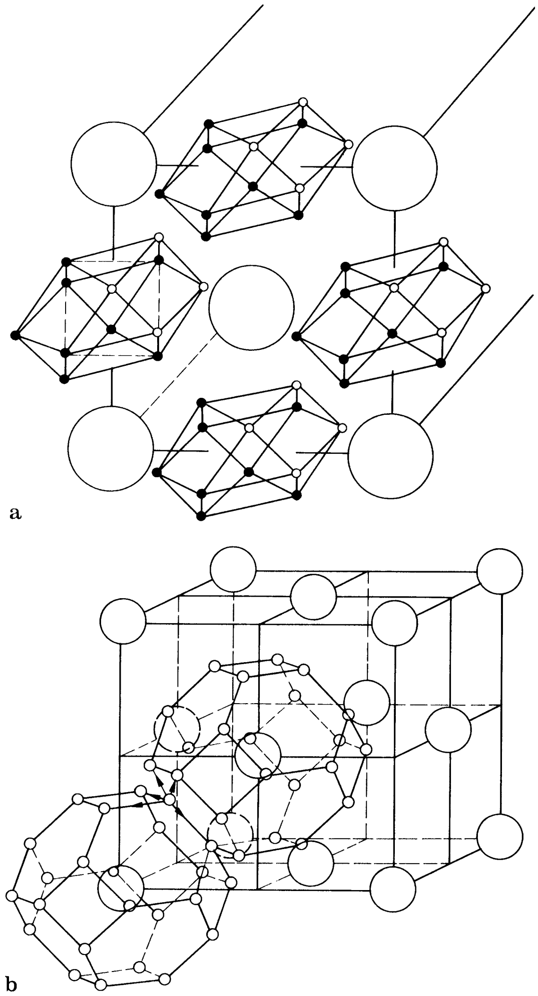

a

b

Fig. 2.

DyB_{12}. Temperature dependence of the electrical resistivity and its derivative. **(a)** Temperature range up to 300 K; **(b)** low temperature range up to 20 K [98G, 99G].

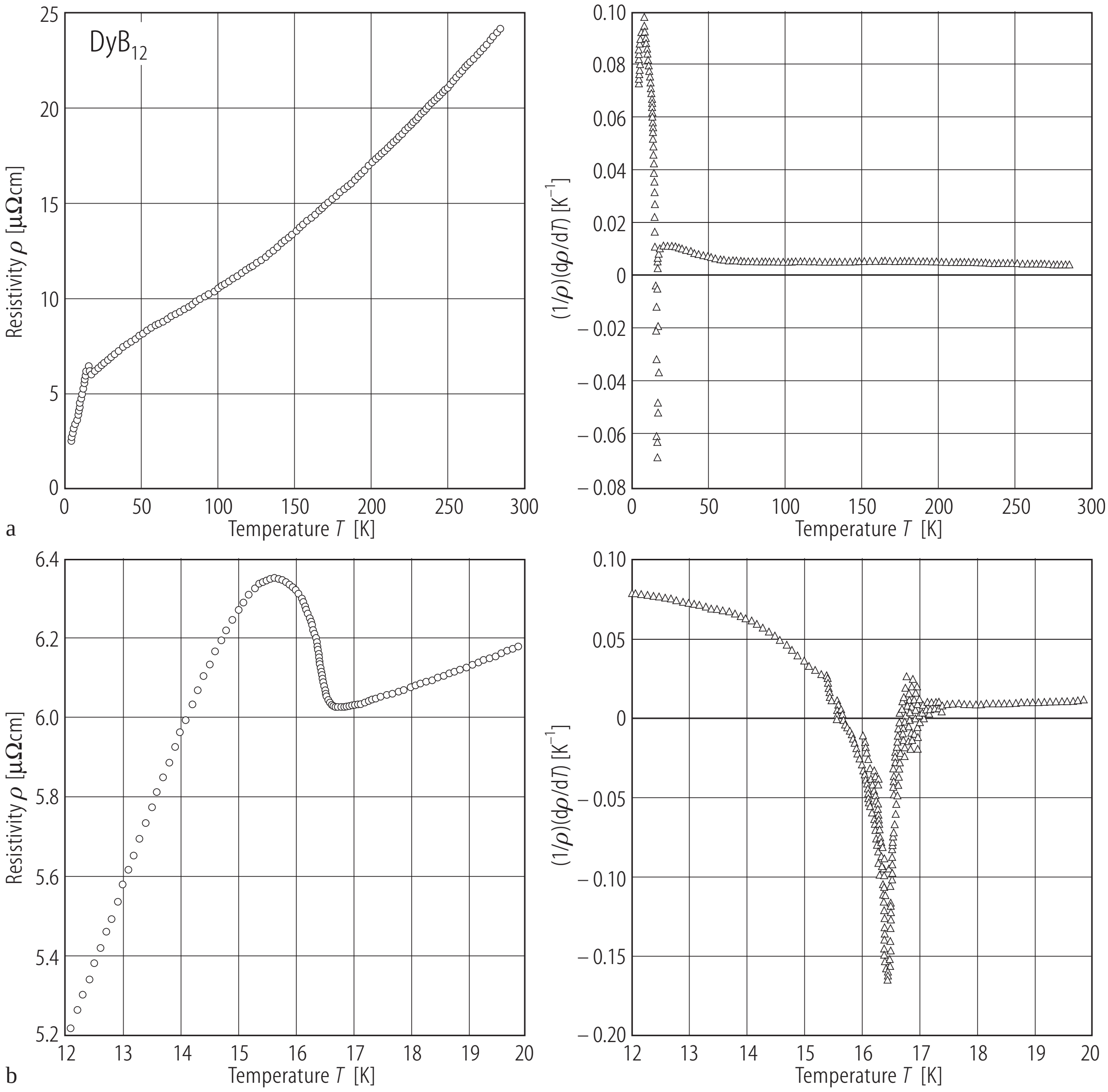

Fig. 3.

Lanthanide dodecaborides. Electrical resistivity vs. T for HoB_{12}, ErB_{12}, TmB_{12}, LuB_{12} [94P]. Error in Fig.: Curves for ErB_{12} and TmB_{12} should be interchanged.

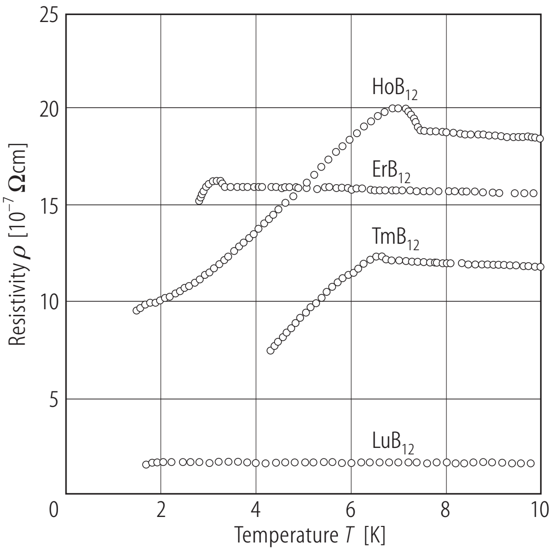

Fig. 4.

HoB_{12}. Temperature dependence of the electrical resistivity and its derivative. **(a)** Temperature range up to 300 K; **(b)** low temperature range up to 9 K [98G, 99G].

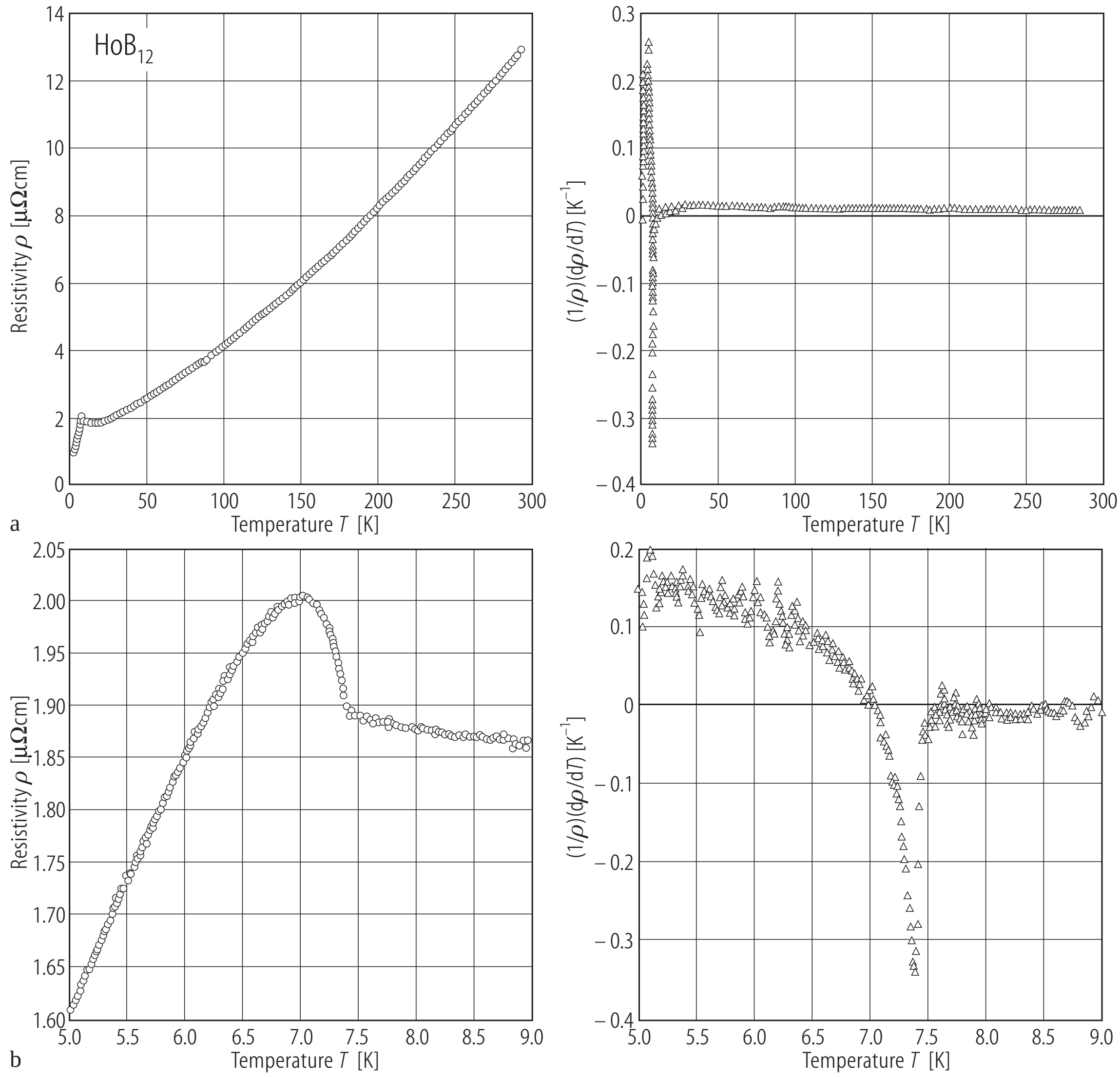

Fig. 5.

HoB_{12}. Reciprocal magnetic susceptibility vs. *T* [94P].

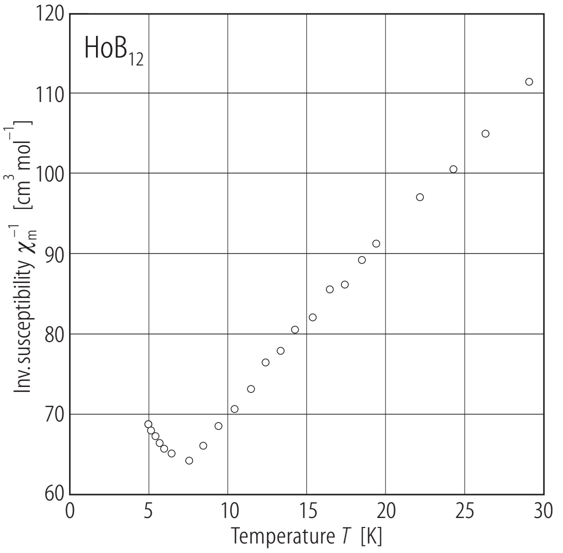

Fig. 6.

ErB_{12}. Temperature dependence of the electrical resistivity and its derivative. **(a)** Temperature range up to 300 K; **(b)** low temperature range up to 8 K [98G, 99G].

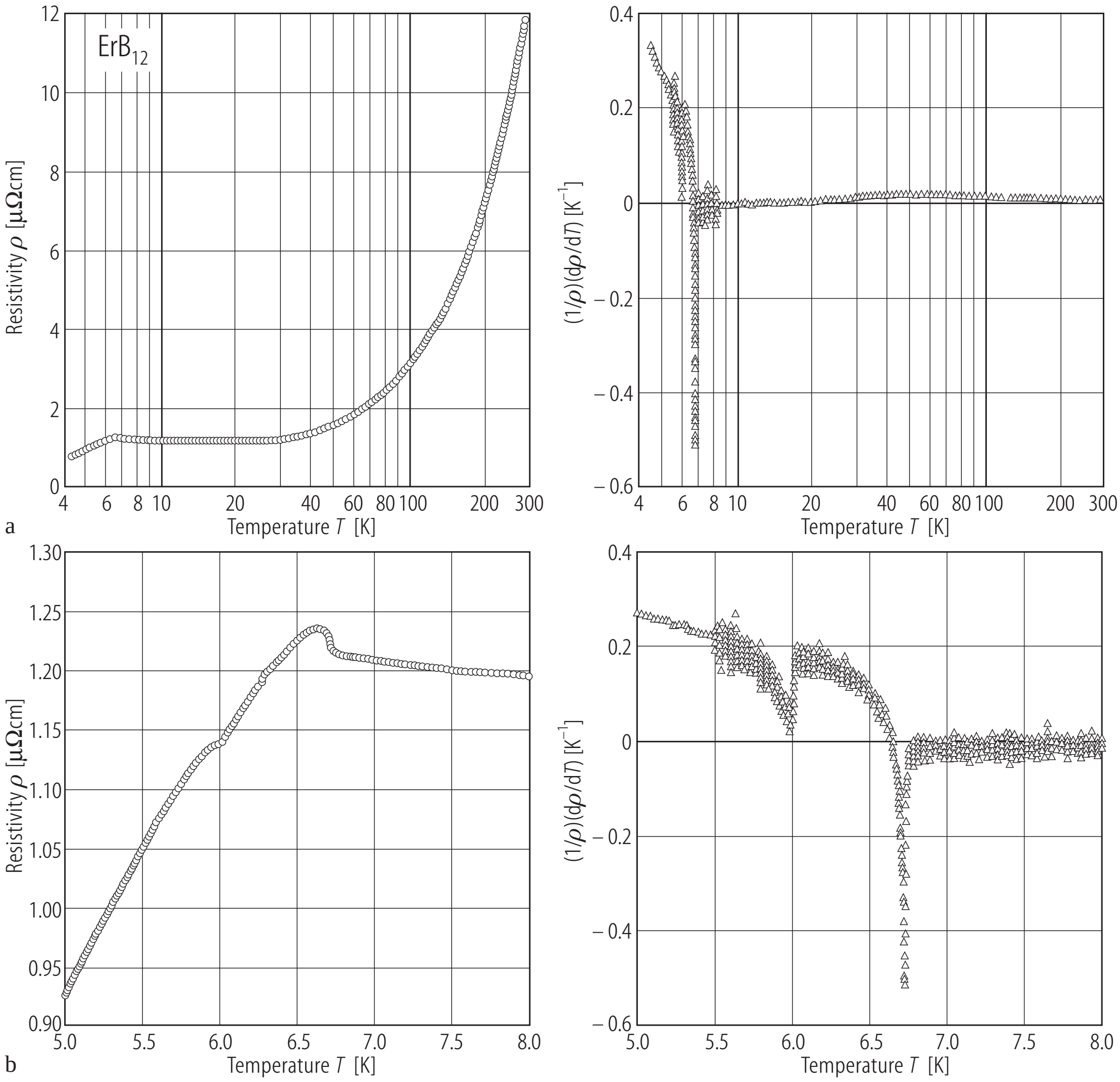

Fig. 7.

TmB_{12}. Anisotropy of the temperature dependence of the electrical resistivity **(a)** and its derivative **(b)** [98G, 99G].

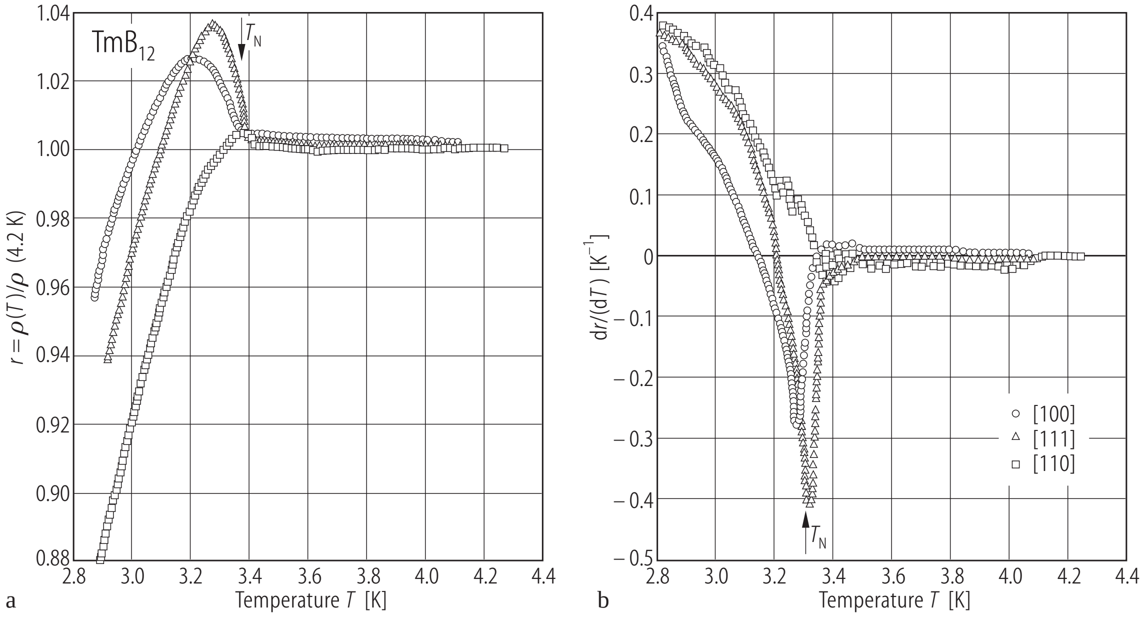

Fig. 8.

YbB_{12}. Thermal expansion vs. *T*; insert: expansion coefficient vs. *T* [87W].

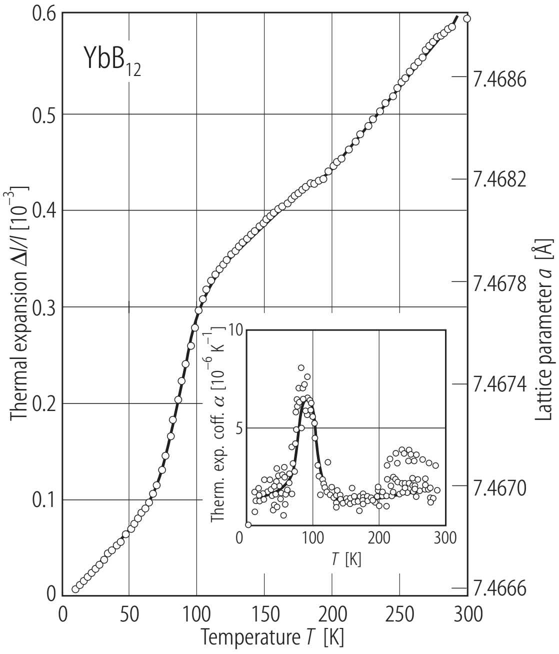

Fig. 9.

YbB_{12}. Magnetic susceptibility, inverse susceptibility,(experimental and theoretical calculation) and Knight shift vs. temperature [87W]. χ_m in CGS-emu.

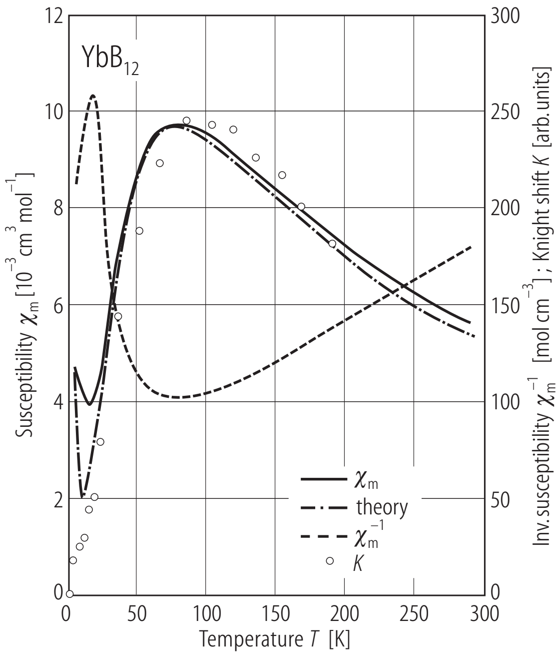

Fig. 10.

LuB_{12}. Temperature dependence of the electrical resistivity and its derivative [95B, 98G, 99G].